Facile One-Pot Preparation of Superparamagnetic Chitosan Sphere and Its Derived Hollow Sphere

Weiwei Zou,[1,2] Hao Geng,[1] Mingfeng Lin,[1] Xiaopeng Xiong[1]

[1]*Department of Materials Science and Engineering, College of Materials, Xiamen University, Xiamen 361005, China*
[2]*Department of Chemistry, College of Chemistry and Chemical Engineering, Xiamen University, Xiamen 361005, China*

Received 21 February 2011; accepted 8 May 2011
DOI 10.1002/app.34887
Published online 21 September 2011 in Wiley Online Library (wileyonlinelibrary.com).

ABSTRACT: A facile and robust approach is presented to prepare superparamagnetic chitosan (CS) spheres by simply dropping iron ions and CS mixture solution to ammonia aqueous solution. Fourier transform infrared spectra, X-ray diffractions, and thermogravimetric analyses of the obtained spheres indicate that the composite spheres consisted of CS and Fe_3O_4. The microstructures of the surface and the inner part of the sphere were observed by scanning electron microscope to indicate nano scale of the Fe_3O_4 component. The results suggest that the nano sized Fe_3O_4 particles can be stabilized by CS molecules in the matrix of sphere to avoid aggregation based on their binding interaction. Because of the nano scale distributed Fe_3O_4 particles, the composite spheres show superparamagnetic properties, and the saturation magnetization of the composite sphere increases linearly with the Fe_3O_4 content. An electron probe microanalyzer was employed to measure the energy dispersive spectra of the magnetic sphere, through which the element contents at different points along the radius of a magnetic CS sphere have been obtained. It has been found that the Fe_3O_4 content decreased gradually from outer surface to its inner core. Moreover, the composite sphere was calcined in air at 700°C to prepare spherical hollow sphere. © 2011 Wiley Periodicals, Inc. J Appl Polym Sci 123: 3587–3594, 2012

Key words: chitosan; nanocomposites; superparamagnetic property; structure-property relations; spherulites

INTRODUCTION

Considerable attention has been focused on organic/inorganic composite materials due to their innovative industrial applications.[1–3] Organic/inorganic composite materials are not simply physical mixtures, and they may be either homogeneous or heterogeneous based on the phase scales of the components. Those materials usually reveal special properties in addition to the sum of the individual contributions. Because of its feasible tunability, polymer is often used for the preparations of organic/inorganic composite materials. The inorganic component is usually inorganic nanoparticles, especially nano sized metal iron oxide. Recently, the magnetite (Fe_3O_4) based magnetic composite materials have stimulated increasing research enthusiasm because of its biocompatibility, high magnetic transition temperature, and high saturation magnetization.[4] If the magnetite composite materials were prepared from biopolymers, their applications in fields such as separation technology, biology, and biomedicine could be expected.

Biocompatible composite materials from magnetite and biopolymers have been widely reported. For examples, Fe_3O_4 particles were adsorbed onto regenerated cellulose matrix to have successfully prepared composite films,[5] fibers,[6] and microspheres.[7] Nano sized hollow particles have also been obtained by self-assembly of chitosan (CS) and Fe_3O_4 particles.[8,9] Moreover, it has been reported that functional groups at the surface of Fe_3O_4 particles could react with those of CS or its derivatives, so that Fe_3O_4 particles were stabilized by layer of polymer coating to obtain nano or micron particles.[10–17] The preparations of such composite materials usually include two steps.[5–17] Firstly, nano sized Fe_3O_4 particles are synthesized by coprecipitation method. Secondly, the nano sized Fe_3O_4 particles are incorporated into polymer matrix. However, the above-mentioned process seems laborious. Strict conditions such as CS derivatives, ultrasonic, microemulsion, and crosslinking are usually required to distribute nano sized Fe_3O_4 particles in polymer matrix evenly. To simplify the preparation, iron and CS mixture solution was dropped directly into ammonia aqueous solution in this work. The composition and

Correspondence to: X. Xiong (xpxiong@xmu.edu.cn).
Contract grant sponsor: National Basic Research Program of China (973 Program); contract grant number: 2010CB732203.
Contract grant sponsor: Fundamental Research Funds for the Central Universities; contract grant number: 2010121055.
Contract grant sponsor: Scientific and Technological Innovation Platform of Fujian Province of China; contract grant number: 2009J1009.

the microstructure of the obtained spheres were studied. The results indicate no aggregation of the *in situ* formed nano Fe_3O_4 particles, but enrichment of the nano Fe_3O_4 particles at the outer surface of the sphere. Magnetic properties of the spheres were measured to show superparamagnetic character. The effect of Fe_3O_4 content on the saturation magnetization (M_s) of the magnetic CS spheres was investigated in detail. Furthermore, hollow iron oxide sphere has been prepared by calcining the obtained composite sphere.

EXPERIMENTAL

Materials

CS, with a degree of deacetylation of 90%, was purchased from Jinan Haidebei Marine Bioengineering Co., Ltd (Shandong, China). The viscosity-average molecular mass (M_η) of CS was determined in a 0.1 mol/L CH_3COONa/0.2 mol/L CH_3COOH buffer at 30°C to be 1.44×10^5 g/mol according to $[\eta] = 6.589 \times 10^{-3} M^{0.88}$.[18] Iron (II) chloride tetrahydrate (99%), iron (III) chloride hexahydrate (97%) and all other reagents are analytical grade, and were purchased from commercial resources in China.

Preparation of magnetic CS spheres

Iron solutions have been prepared by dissolving iron (II) chloride tetrahydrate and iron (III) chloride hexahydrate in distilled water, in which the molar ratio of Fe^{3+} : Fe^{2+} was kept stoichiometrically constant as 2 : 1. CS was dissolved in 2 wt % acetic acid aqueous solution to have a 5 wt % polymer concentration. Then, the iron solution with desired concentration and the CS solution were mixed according to the solution weight ratio of 1 : 1 or 2 : 1, which was dropped with a syringe through a needle into a 25% ammonia aqueous solution under stirring at room temperature. After about 1.5 h, the slurry was filtered, and then washed totally with distilled water, and finally vacuum dried at 50°C to obtain the magnetic CS spheres (MCSS). The final sphere codes and their preparation conditions such as starting iron (III) concentration before mixing ($c_{Fe(III)}$) and the CS concentration in the mixture solution (c_{CS}) are listed in Table I. The obtained magnetic CS spheres were heated by a programmed speed from room temperature to 700°C in a muffle to prepare hollow spheres.

Characterizations

Fourier transform infrared (FTIR) spectra of the magnetic CS spheres were recorded with a Fourier transform infrared spectrometer (Nicolet AVATAR 360, Pittsfield, USA) at 25°C. The spheres were firstly ground, and then were vacuum-dried at 40°C for over 48 h to mix with KBr to produce disks for the measurements.

TABLE I
The Final Sphere Codes, the Preparation Conditions Such as Starting Iron (iii) Concentration Before Mixing ($c_{Fe(III)}$) and the CS Concentration in the Mixture Solution (c_{CS}). The Fe_3O_4 Content (w_{Fe3O4}) and the Saturation Magnetization (M_s) of the Magnetic Spheres Are also Included in the Table.

Codes	c_{CS} (wt %)	$c_{Fe(III)}$ (mol/L)	w_{Fe3O4} (%)	M_s (emu)
MCSS1	2.5	1	55.1	44.2
MCSS2	2.5	0.25	39.5	22.0
MCSS3	2.5	0.1	21.5	11.8
MCSS4	1.7	1	71.2	49.8
MCSS5	1.7	0.25	53.6	36.3
MCSS6	1.7	0.1	33.9	22.2

X-ray diffraction (XRD) was carried out by using a PANalytical X'Pert PRO diffractometer (PANalytical, The Netherlands) with CuKα radiation. The ground spheres were continuously scanned from10° to 70° (2θ) at a speed of 0.0167°/s.

Thermogravimetric analyses (TGA) for the spheres were performed on a NETZSCH409EP thermal analyzer (Netzsch, Germany) under nitrogen atmosphere at a heating speed of 20 °C/min from 25 to 700°C.

The magnetic CS spheres before drying were cut into halves with a surgery knife, then were frozen in liquid nitrogen, and finally were vacuum-dried. The spheres sintered at 700°C were crushed mechanically. The surface and cross-section of the samples were coated with a thin layer of gold (about 2 nm) to observe their microstructures by using an electron probe microanalyzer instrument (EPMA, JXA-8100, JEOL, Japan) with 15 kV accelerating voltage. The elemental distribution along radius of the magnetic sphere was also examined with the instrument by using an energy dispersive spectrometer (EDS).

A vibrating sample magnetometer VSM-5-15, (TOEI Industry Co., Ltd, Japan) was used to assess the magnetic properties of the spheres. Certain amount of the spheres was positioned in the magnetometer and was balanced before measurements. The hysteresis of the magnetization was determined by increasing magnetic field intensity (H) from −20000 Oe to + 20000 Oe at 27°C, and the magnetic properties for the spheres were evaluated in terms of saturation magnetization (M_s) and coercivity.

RESULTS AND DISCUSSION

Composition of magnetic CS spheres

Figure 1 shows the FTIR spectra of pure CS and of the magnetic spheres. For pure CS, the peaks at

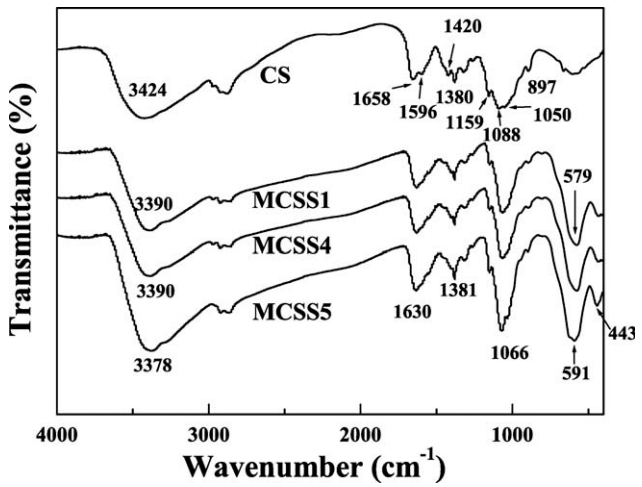

Figure 1 FTIR spectra of the pure CS and of the magnetic spheres of MCSS1, MCSS4, and MCSS5.

around 897 and 1159 cm^{-1} in the FTIR spectra are assigned to its saccharide structure, and its C—O—C functional groups are found at 1050 and 1088 cm^{-1}. The characteristic bands of amide-I, amide-II, and amide-III for CS can be found at 1658, 1596, and 1380 cm^{-1}, respectively. The peak at 1420 cm^{-1} is attributed to the -NH deformation vibration of the amine groups belonging to CS. For magnetic spheres, their spectra are similar and most of the characteristic bands of the polysaccharide are constant, except that some peaks shift to lower or to higher frequencies. Moreover, the FTIR spectra of magnetic spheres exhibit strong and broad bands in the low frequency region below 800 cm^{-1}, which is consistent with that of magnetite Fe_3O_4.[15] The XRD patterns of pure CS and MCSS1 are shown in Figure 2. It is seen that the pattern of pure CS reveals only broad diffraction at 2θ around 19.8°, while that of MCSS1 exhibits six characteristic peaks at 2θ = 30.1°, 35.5°, 43.1°, 53.4°, 57.0°, and 62.6°, corresponding to the diffraction planes of, (220), (311), (400), (422), (511), and (440) of spinel structured Fe_3O_4,[9] respectively. At the same time, it has been found that the presence of Fe_3O_4 in the CS matrix might interfere with the crystallization of CS, resulting in the disappearance of the diffraction peak of CS in the XRD pattern of the MCSS1. Those results indicate the magnetic spheres are consisted of CS and Fe_3O_4.

The acidic mixture solution of iron and CS was added dropwise into alkali ammonia solution, so that the CS and the Fe ions could be precipitated accordingly. It has been suggested[5–17] that the Fe ions in the drop were transformed into Fe_3O_4, so its content in the final magnetic sphere could be determined experimentally by TGA measurements. The thermograms of the spheres are shown in Figure 3. The pure CS sphere exhibits three obvious stages of weight losses, and the composite spheres display similar thermal behaviors. The weight losses for all the spheres are quite low below 230°C, which might be due to the removal of water absorbed physically or chemically. In the second stage between 230°C and 315°C, the weight losses are much higher because of the thermal decomposition of CS[19,20] in the spheres. At temperature higher than 315°C, CS decompose further, and the weight losses of the composite spheres are attributed to the degradation of the CS that binds with Fe_3O_4 particles.[12] When the temperature was raised to higher than 639°C, there was no significant weight change for pure CS, indicating complete decomposition of CS. The ash content of CS is thus found to be 1.9%. For composite spheres, constant weight residues were found to be started at lower temperatures, suggesting the presence of only iron oxide and ash. The weight loss below 639°C is thus estimated to be the absorbed water and the CS in a

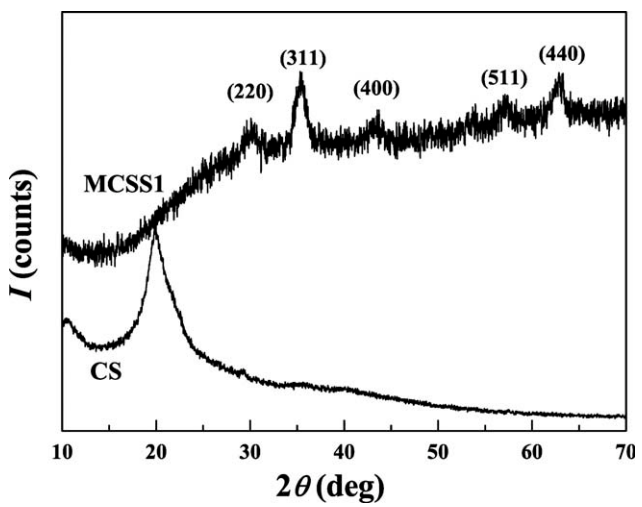

Figure 2 The XRD patterns of pure CS and MCSS1.

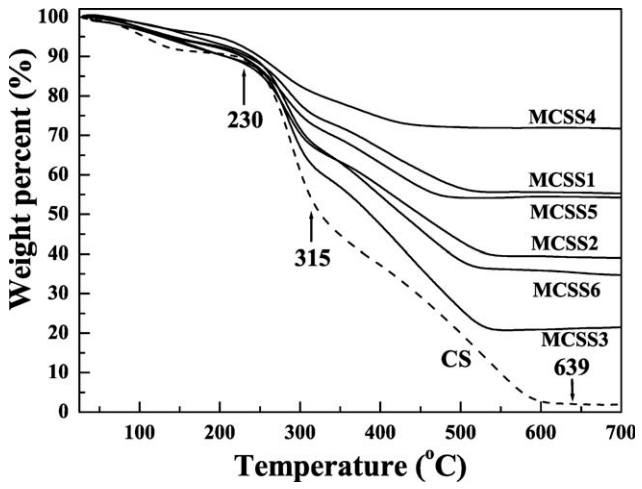

Figure 3 TGA curves of the spheres. The arrows indicate the specific temperatures.

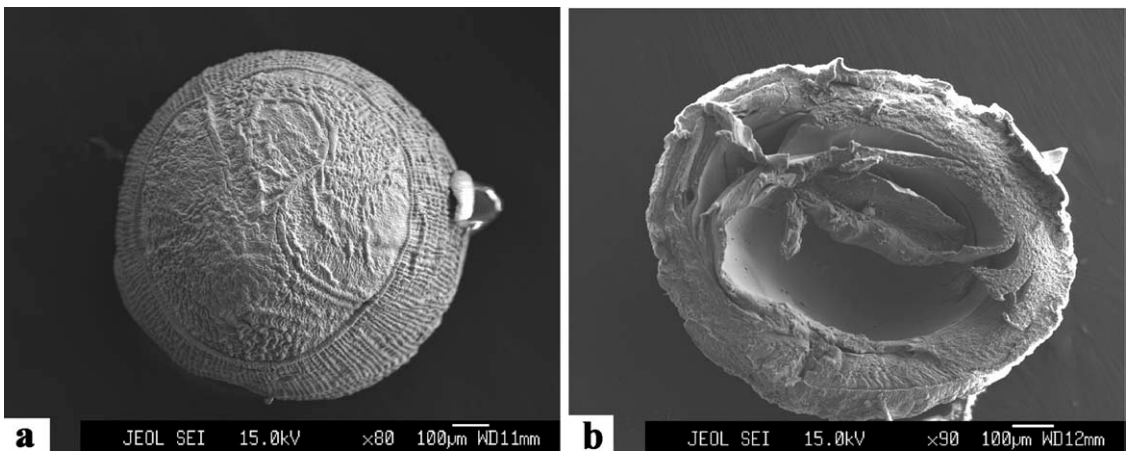

Figure 4 SEM images of the surface (a) and inner part (b) of MCSS1.

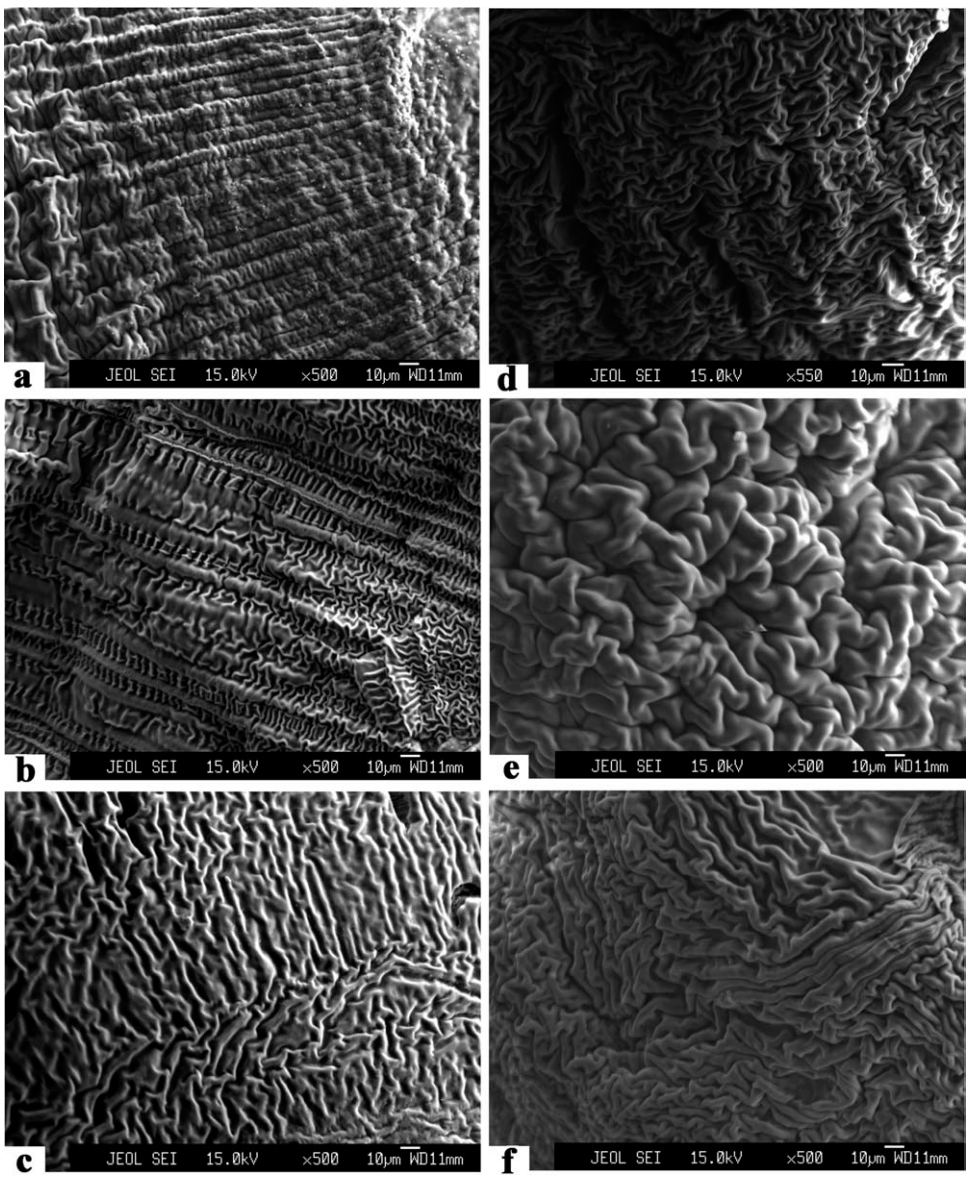

Figure 5 SEM images of the magnetic spheres prepared from 2.5 wt % (left column) and 1.7 wt % (right column) CS solutions with different iron content: (a) MCSS1; (b) MCSS2; (c) MCSS3; (d) MCSS4; (e) MCSS5; (f) MCSS6.

sphere, so that the Fe_3O_4 contents (w_{Fe3O4}) in the magnetic spheres can be calculated. The Fe_3O_4 contents of the magnetic spheres are summarized in Table I. It is therefore found that the Fe_3O_4 content in the sphere increases with initial iron concentration, and can be tuned easily by changing the initial amount of Fe ions.

Microstructure

The obtained wet spheres are about 1.5 mm in diameter, and they decrease to around 1 mm after drying. The scanning electron microscope (SEM) images of the surface and of the inner frozen-dried MCSS1 are shown in Figure 4. It can be seen that the obtained material is spherical shape, and the surface of the magnetic sphere is compact and wrinkle or stripe-like microstructure. The inner part of the sphere reveals multilayer structure, and each layer exhibits dense morphology, which is similar as the multi-membrane hydrogels of CS reported by Ladet et al.[21] The compact wrinkle or stripe-like structure of the surface might be due to the immediate precipitation of CS molecules in alkali ammonia solution coagulant and to the subsequent shrinking of the sphere resulted from drying. The multi-layered cross-section was possibly caused by multi-step of solvent exchange.[21] However, it is interesting to find that there is no obvious phase separation in each layer even in SEM image with a much higher magnification, indicating that Fe_3O_4 component are at the scale of nano size. The results imply that the nano sized Fe_3O_4 particles were embedded and stabilized in the CS matrix.

The stabilization of nano sized Fe_3O_4 particles by CS can also be evidenced by the FTIR spectra of magnetic spheres. In Figure 1, it can be seen that the band of amide-I for CS shifts to 1630 cm^{-1}, and the amide-II at 1596 cm^{-1} is not obvious in the spectra of magnetic spheres. At the same time, the -NH deformation vibration of the amine groups at 1420 cm^{-1} for pure CS almost disappears, and the band around 3420 cm^{-1} for hydrogen-bonded O—H and *N*—H stretching vibrations shift to lower frequencies of below 3400 cm^{-1}. Those results indicate strong interactions between CS and nano sized Fe_3O_4 particles,[11,14,15,22] which benefits the stabilization of the nano Fe_3O_4 particles by the neighboring CS molecules and prevents them from aggregating. Kim and coworkers[15] suggest that the potential sites of CS to bind with nano sized Fe_3O_4 particles could be the free amine group and the carbonyl oxygen (*N*—C=O). Moreover, the nano scaled Fe_3O_4 particles interacted with CS matrix to interfere with the crystallization of CS, which is evidenced in Figure 2.

The surface morphologies of the other magnetic spheres are similar as that of MCSS1. However, the concentrations of CS and of iron in the starting mixture solution may influence the morphologies of the final magnetic spheres. Figure 5 shows SEM images of the magnetic spheres prepared from 2.5 wt % (left column) and 1.7 wt % (right column) CS solutions with different iron content. It can be seen that the wrinkles and stripes are bigger when the spheres are prepared from lower concentration of CS solution. Similarly, the lower starting iron concentration will lead to bigger wrinkles and stripes of the obtained sphere. It can be conceived that the CS molecules

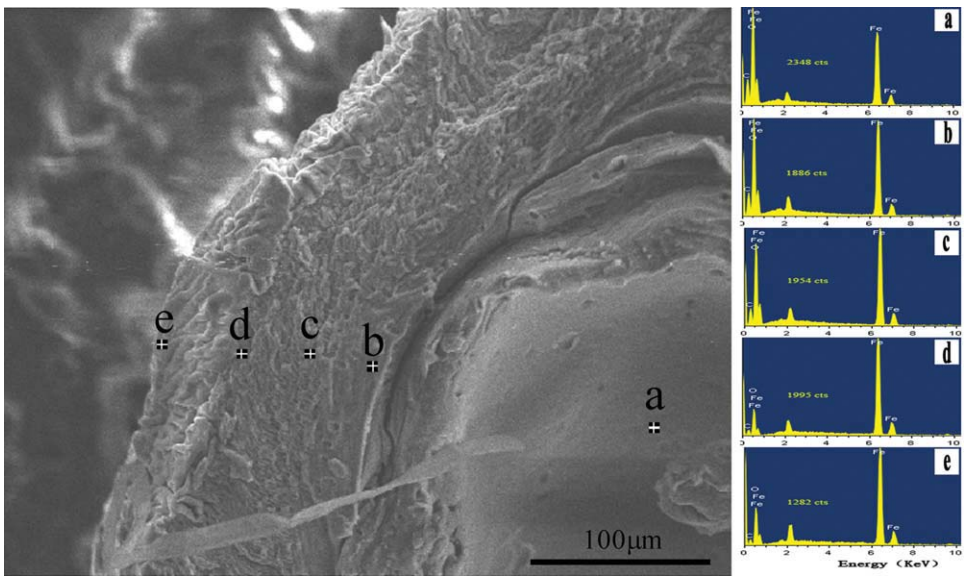

Figure 6 SEM image showing the points of MCSS1 along its radius examined by EDS (left part) and their EDS spectra (right part). [Color figure can be viewed in the online issue, which is available at wileyonlinelibrary.com.]

TABLE II
The Element Contents of the Points Shown in Figure 6, Which Were Directly Obtained from EDS Spectra

Position	Fe (%)	O (%)	C (%)
a	43.3	37.3	19.4
b	50.9	32.8	16.3
c	56.2	29.3	14.6
d	79.0	13.2	7.8
e	75.9	17.0	7.1

would be immediately precipitated to form hydrogel when the mixture solution drop touched the alkali ammonia solution coagulant. At the same time, the Fe ions could be precipitated to form nano sized Fe_3O_4, which was stabilized by CS matrix in the hydrogel as mentioned above. The subsequent drying would probably lead to shrinking of the hybrid hydrogel, resulting in wrinkle and stripe-like surface morphology of the sphere. With higher CS concentration, the obtained hydrogel would be denser, and its shrinkage would be smaller. Similarly, the shrinkage of the formed hydrogel would be prevented by a higher content of Fe_3O_4 particles in the matrix, which could be considered as cross-links due to the binding interaction. As a result, the wrinkles and stripes would get bigger with the concentration decrease of both CS and iron solution. The wrinkle and stripe-like surface morphology would provide the sphere relatively high specific area, meaning potential applications of the magnetic sphere in many fields.

The distribution of the nano sized Fe_3O_4 particles in a composite sphere was analyzed by determining the iron element along its radius. The parts examined by EDS are marked in the SEM image of MCSS1 (Fig. 6, left part). From the EDS spectra of the points (Fig. 6, right part), the element contents of Fe, C, and O can be calculated by comparing the corresponding peak areas, and the results are summarized in the Table II. It is therefore found that the element Fe is not evenly distributed in the sphere. In other words, the content of the nano sized Fe_3O_4 particles increases from inner part to surface of the sphere. The uneven distribution of the Fe_3O_4 particles in the composite sphere has been understood as following: when the CS solution was blended with the solution of Fe ions, the mixture solution was homogeneous; after dropping the mixture solution to ammonia aqueous solution, the CS molecules at the surface of the solution drop were precipitated immediately to form hydrogels based on the drastic neutralization reaction of the solvents; at the same time, the Fe ions at the surface could also be precipitated to form nano sized Fe_3O_4 particles and to bestabilized by the precipitated CS hydrogel at the surface; because the hydrogel at the surface would slow down the diffusion of small molecules, the neutralization reaction of the solvents would be slowed accordingly; the slowed neutralization reaction would lead to the diffusion of Fe ions from inner part of the solution drop to the outer, which was evidenced by the higher Fe content at position *d* than that at the extremely outer position *e*, and by the gradual decrease of Fe content at positions from *d* to *a*. The multilayer structure of the sphere might contribute to unequal distribution of nano sized Fe_3O_4 particles as well.

Magnetic property

The magnetic properties of the spheres were measured by a vibrating sample magnetometer. The

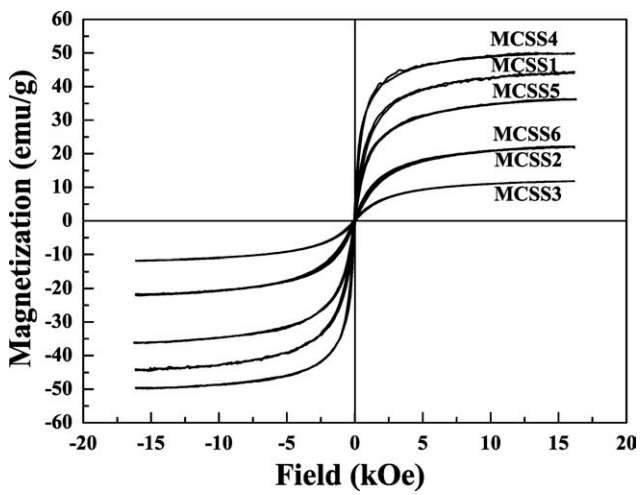

Figure 7 The hysteresis loops of the spheres at 27°C.

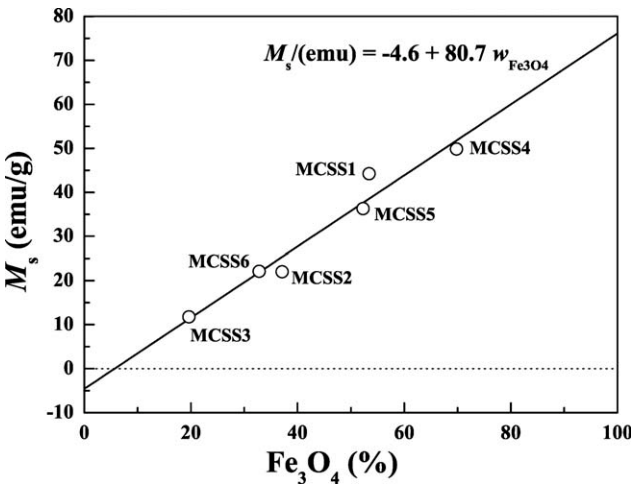

Figure 8 The dependence of M_s on the Fe_3O_4 content in magnetic sphere. The full line (M_s/(emu) = −4.6 + 80.7 w_{Fe3O4}) is the linear fit of the data points obtained from Figure 7 and the doted line is zero emu/g.

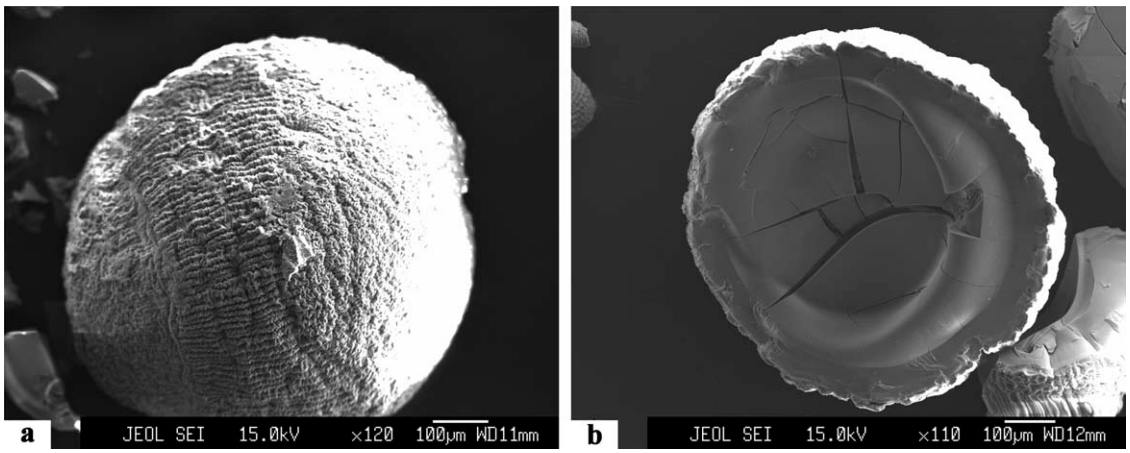

Figure 9 SEM images of MCSS1 after calcined at 700°C in air.

hysteresis loops are shown in Figure 7. As revealed in the figure, the invisible hystereses suggest superparamagnetic materials of all the spheres. It is known that the character of ideal superparamagnetic materials with size less than 20 nm is zero coercivity and zero remanence. The result indicates that the nano Fe_3O_4 particles in the present magnetic spheres were less than 20 nm, which is consistent with the results mentioned above. The M_s values of the magnetic CS spheres determined from the hysteresis loops are summarized in Table I. The dependence of M_s on Fe_3O_4 content is shown in Figure 8, displaying almost linear increase of the M_s on the Fe_3O_4 content in the sphere by a manner of $M_s/(\text{emu}) = -4.6 + 80.7\ w_{Fe3O4}$. It is interesting to deduce that the M_s of pure Fe_3O_4 nanoparticles was 76.1 emu/g, which is at the same level as those reported in literatures.[10–17] On the other side, the M_s of pure CS could be obtained by extending the line to zero Fe_3O_4 content to be −4.6 emu/g, suggesting diamagnetic contribution of the CS that was binding with Fe_3O_4 nanoparticles[13] in the spheres. The results mean that superparamagnetic CS spheres with desired saturation magnetization could be easily prepared.

Hollow sphere

The enrichment of nano Fe_3O_4 particles at the outer surface indicates the possibility to prepare hollow spheres from the composite magnetic sphere. The magnetic CS sphere of MCSS1 was thus calcined in a muffle furnace at 700°C. From the results of TGA measurements, it can be shown that the CS in the spheres could be thermally decomposed at this temperature totally, and the residue would be iron oxide. Figure 9 shows the morphologies of the sphere MCSS1 after calcination. It is found that the calcined material retains spherical shape (Fig. 9, left part). At the same time, clear concavity in the central part of a half sphere and arc shaped fragment are found for broken spheres (Fig. 9, right part). These observations suggest the hollow morphology of the calcined spherical particles. The wrinkle and stripe-like surface morphology is kept constant after calcination, but the inner surface displays dense concrete microstructure.

CONCLUSIONS

Magnetic CS spheres have been prepared by dropping iron and CS mixture solution to ammonia aqueous solution. The FTIR, TGA, and XRD analyses indicate that the composite spheres consisted of CS and Fe_3O_4. The SEM observation suggests that the surfaces of the magnetic spheres are compact wrinkle and stripe-like microstructure, and the wrinkles and stripes become bigger with decrease of either the initial iron concentration or the CS concentration. The inner part of the magnetic sphere reveals multilayered structure, and no obvious phase separation has been found, indicating nano scale of the Fe_3O_4 component. Due to the binding interactions, the nano sized Fe_3O_4 particles can be stabilized by the CS molecules in the sphere matrix to avoid aggregation. Because of the nano scaled Fe_3O_4 particles, the composite spheres show superparamagnetic properties. The saturation magnetization increases linearly with the Fe_3O_4 content in the composite sphere by a manner of $M_s/(\text{emu}) = -4.6 + 80.7\ w_{Fe3O4}$, meaning that superparamagnetic CS spheres with desired saturation magnetization could be easily prepared. Element analysis along the radius of a composite sphere demonstrates that the content of Fe_3O_4 decreases from outer surface to inner core. Based on the enrichment of Fe_3O_4 particles at the outer surface, the magnetic sphere was subjected to calcination at 700°C to obtain spherical hollow sphere. The magnetic CS sphere and the hollow iron oxide sphere

might have potential applications in fields such as waste water treatment, drug delivery, catalyst carrier, and so on.

References

1. Sanchez, C.; Julián, B.; Belleville, P.; Popall, M. J Mater Chem 2005, 15, 355.
2. Xu, X.; Wang, X. J Mater Chem 2009, 19, 3572.
3. Kabiri, K.; Omidian, H.; Zohuriaan-Mehr, M. J.; Doroudiani, S. Polym Compos 2011, 32, 277.
4. Cornell, R. M.; Schwertmann, U. The Iron Oxide: Structure, Properties, Reactions, Occurrence and Uses; VCH: Germany, 1996.
5. Liu, S.; Zhou, J.; Zhang, L.; Guan, J.; Wang, J. Macromol Rapid Commun 2006, 2084, 27.
6. Liu, S.; Zhang, L.; Zhou, J.; Xiang, J.; Sun, J.; Guan, J. Chem Mater 2008, 20, 3623.
7. Luo, X.; Liu, S.; Zhou, J.; Zhang, L. J Mater Chem 2009, 19, 3538.
8. Ding, Y.; Hu, Y.; Jiang, X.; Zhang, L.; Yang, C. Angew Chem Int Ed 2004, 43, 6369.
9. Mu, B.; Liu, P.; Dong, Y.; Lu, C.; Wu, X. J Polym Sci Part A: Polym Chem 2010, 48, 3135.
10. Denkbaş, E. B.; Kiliçay, E.; Birlikseven, C.; Öztürk, E. React Funct Polym 2002, 50, 225.
11. Park, J.-H.; Im, K.-H.; Lee, S.-H.; Kim, D.-H.; Lee, D.-Y.; Lee, Y.-K.; Kim, K.-M.; Kim, K.-N. J Magn Magn Mater 2005, 293, 328.
12. Zhi, J.; Wang, Y.; Lu, Y.; Ma, J.; Luo, G. React Funct Polym 2006, 66, 1552.
13. Chang, Y.-C.; Chang, S.-W.; Chen, D.-H. React Funct Polym 2006, 66, 335.
14. Yang, P.-F.; Lee, C.–K. Biochem Eng J 2007, 33, 284.
15. Bhattarai, S. R.; Bahadur, K. C. R.; Aryal, S.; Khil, M. S.; Kim, H. Y. Carbohydr Polym 2007, 69, 467.
16. Peniche, H.; Osorio, A.; Acosta, N.; de la Campa, A.; Peniche, C. J Appl Polym Sci 2005, 98, 651.
17. Guo, J.; Wang, C.; Mao, W.; Yang, W.; Liu, C.; Chen, J. Nanotechnology 2008, 19, 315605.
18. Xiong, X.; Duan, J.; Zou, W.; He, X.; Zheng, W. J Membr Sci 2010, 363, 96.
19. Wan, Y.; Wu, H.; Yu, A.; Wen, D. Biomacromolecules 2006, 7, 1362.
20. Tang, W.; Wang, C.; Chen, D. Polym Degrad Stab 2005, 87, 389.
21. Ladet, S.; David, L.; Domard, A. Nature 2008, 452, 76.
22. Klepka, M. T.; Nedelko, N.; Greneche, J.-M.; Lawniczak-Jablonska, K; Demchenko, I. N.; Slawska-Waniewska, A.; Rodrigues, C. A.; Debrassi, A.; Bordini, C. Biomacromolecules 2008, 9, 1586.